

**THE TEMPERATURE SCALE OF METAL-RICH M GIANTS  
BASED ON TiO BANDS: POPULATION SYNTHESIS IN THE  
NEAR INFRARED <sup>1</sup>**

**R. P. Schiavon<sup>2,3</sup>, B. Barbuy<sup>2</sup>**

Received \_\_\_\_\_; accepted \_\_\_\_\_

Send proofs to: R. P. Schiavon

---

<sup>1</sup>Observations obtained at the Laboratório Nacional de Astrofísica (LNA), Brazil, and European Southern Observatory (ESO), Chile

<sup>2</sup>Universidade de São Paulo, IAG, Departamento de Astronomia, C.P. 3386, São Paulo 01060-970, Brazil, Email: ripisc@on.br, barbuy@orion.iagusp.usp.br

<sup>3</sup>Present Address: CNPq/Observatório Nacional, Departamento de Astronomia, Rua General José Cristino, 77, Rio de Janeiro, 20921-400, Brazil.

## ABSTRACT

We have computed a grid of high resolution synthetic spectra for cool stars ( $2500 < T_{eff} < 6000$  K) in the wavelength range  $\lambda\lambda$  6000 – 10200 Å, by employing an updated line list of atomic and molecular lines, together with state-of-the-art model atmospheres.

As a by-product, by fitting TiO bandheads in spectra of well-known M giants, we have derived the electronic oscillator strengths of the TiO  $\gamma'$ ,  $\delta$ ,  $\epsilon$  and  $\phi$  systems. The derived oscillator strengths for the  $\gamma'$ ,  $\epsilon$  and  $\phi$  systems differ from the laboratory and ab initio values found in the literature, but are consistent with the model atmospheres and line lists employed, resulting in a good match to the observed spectra of M giants of known parameters.

The behavior of TiO bands as a function of the stellar parameters  $T_{eff}$ ,  $\log g$  and  $[\text{Fe}/\text{H}]$  is presented and the use of TiO spectral indices in stellar population studies is discussed.

*Subject headings:* Atomic and molecular data, Stars: atmospheres, M giants, globular clusters

## 1. INTRODUCTION

A series of TiO spectral features are present in the integrated spectra of normal galaxies. Measurements of  $\text{TiO}_1$  and  $\text{TiO}_2$  indices as defined in Burstein et al. (1984) and Worthey et al. (1994), and several indices given in Bica & Alloin (1986) are available in the literature. However, the use of TiO bands as stellar population indicators is not widespread.

One clear characteristic of TiO bands is the dependence of their intensity on effective temperature. The effective temperature ( $T_{\text{eff}}$ ) scale of M giants has been the subject of many studies in the past, both from the theoretical and observational standpoints – see the recent work by Bessell et al. (1998, hereafter BCP98) and Lejeune et al. (1998). The main source of uncertainty in the temperature scale of M giants is related to uncertainties in the stellar mass, surface gravity and metallicity (Alvarez & Plez 1998).

In this work, we use a revised atomic and molecular line list and state-of-the-art model atmospheres to synthesize the spectra of M giants in the near-infrared (NIR). A comparison of synthetic spectra with observations of cool red giants permits a calibration of  $T_{\text{eff}}$ s for cool giants of the bulge metal-rich globular cluster NGC 6553.

A grid of synthetic spectra in the wavelength range  $\lambda\lambda$  6000 – 10200 Å is computed and equivalent widths of TiO bands as a function of stellar parameters ( $T_{\text{eff}}$ ,  $\log g$ ,  $[\text{Fe}/\text{H}]$ ) are measured.

In Sec. 2 the observations are reported. In Sec. 3 the calculation of synthetic spectra is described. In Sec. 4 we derive effective temperatures for M giants of the globular cluster NGC 6553, based on the intensity of NIR TiO bands, and we derive electronic oscillator strengths for the TiO  $\gamma'$ ,  $\delta$ ,  $\epsilon$  and  $\phi$  systems. In Section 5 the computation of a grid of synthetic spectra in the NIR and measurements of equivalent widths of TiO features are presented; using the grid of synthetic spectra, the composite spectrum for a single-age

stellar population is built and compared to the observed integrated spectrum of the globular cluster NGC 6553. In Section 6 conclusions are drawn.

## 2. OBSERVATIONS

We have observed 6 stars among the coolest giants of the bulge metal-rich globular cluster NGC 6553 and two well-known field M giants HR 625 and HR 3816. The selection and identification of the stars in NGC 6553 were based on the images and Colour-Magnitude Diagrams (CMDs) given in Ortolani et al. (1990) and Guarnieri et al. (1998). The list of stars is shown in Table 1.

The spectra of individual stars from the RGB tip of NGC 6553 were collected at the Cassegrain focus of the 1.6m telescope at the *Laboratório Nacional de Astrofísica* (LNA), Pico dos Dias, Brazil, in 1997 June, using a EEV CCD of  $770 \times 1152$  pixel (LNA CCD # 48) of pixel size  $22.5 \mu\text{x}22.5 \mu\text{m}$ , and a grating of 830l/mm, with blaze angle at 7490 Å. This combination gives a spectral resolution of  $\Delta\lambda \sim 3$  Å, centered at  $\lambda 8000$  Å with a spectral coverage of  $\Delta\lambda \sim 1350$  Å. In order to enlarge the spectral interval to include bands from all the relevant electronic transitions of TiO, we collected two spectra for each star, centered at  $\lambda 7570$  and  $\lambda 8235$  Å with an overlap in the interval  $\lambda \lambda 7570\text{--}8250$  Å. At the end of the reduction process, the spectra were combined and the final spectral interval is  $\lambda \lambda 6865\text{--}8905$  Å. The flux calibration shows a systematic turnover around  $\lambda 8700$  Å, which affects the spectrum shape at the  $< 5\%$  level. The effect of this photometric inaccuracy on relative band intensities is negligible.

An integrated spectrum of NGC 6553 and the M giant HR 625 were observed at LNA in 1996 July and in 1996 August respectively, at the Cassegrain focus of the 1.6m telescope, using a grating of 300l/mm, with blaze angle at  $\lambda 10000$  Å. Employing a  $1024 \times 1024$  pixels

thin back-illuminated SITe CCD (LNA CCD # 101), of pixel size  $24\mu\text{m}\times 24\mu\text{m}$ , a spectral coverage  $\lambda\lambda 6020 - 10380 \text{ \AA}$ , with an effective resolution of  $8\text{ \AA}$ , was obtained.

The M giant HR 3816 was observed in 1996 February at the 1.5m telescope of the *European Southern Observatory* - ESO using the Ford Aerospace ESO CCD # 24, of  $2048\times 2048$  pixels, with pixel size  $15\mu\text{m}\times 15\mu\text{m}$ , together with a grating of 1200 l/mm (ESO grating # 11), giving a dispersion of  $66 \text{ \AA}/\text{mm}$  or a spectral resolution of  $\Delta\lambda \sim 2 \text{ \AA}$ .

Reductions were carried out using IRAF, following the usual steps: bias subtraction, flat-field and illumination correction, spectrum extraction and wavelength calibration. The spectra were flux calibrated through observations of three spectrophotometric standards per night, taken from Hamuy et al. (1994). Telluric lines have been removed through division by spectra of high  $v \sin i$  B stars.

### 3. SPECTRUM SYNTHESIS

A grid of synthetic spectra in the wavelength range  $\lambda\lambda 6000 - 10200 \text{ \AA}$  is computed, using a revised version (Barbuy, B., Perrin, M.-N., in preparation) of the code described in Barbuy (1982), which incorporates the computation of molecular lines to the code for atomic lines by Spite (1967), assuming local thermodynamic equilibrium. The elemental abundances adopted are from Grevesse et al. (1996). The atomic lines are identified in the solar spectrum and oscillator strengths are obtained through a fit of synthetic spectra to the solar spectrum (Delbouille et al. 1973). The molecular systems taken into account are the CN ( $A^2\Pi-X^2\Sigma$ ) red system,  $C_2$  ( $A^3\Pi_g-X^3\Pi_u$ ) Swan system, TiO  $\gamma$  ( $A^3\Phi-X^3\Delta$ ),  $\gamma'$  ( $B^3\Pi-X^3\Delta$ ),  $\delta$  ( $b^1\Pi-a^1\Delta$ ),  $\epsilon$  ( $E^3\Pi-X^3\Delta$ ) and  $\phi$  ( $b^1\Pi-d^1\Sigma$ ) systems, and the FeH ( $A^4\Delta-X^4\Delta$ ) electronic system, which contains the Wing-Ford band.

The detailed study of the  $C_2$  Swan, CN red and TiO  $\gamma$  systems and respective molecular

constants employed can be found in Barbuy (1985), Erdelyi-Mendes & Barbuy (1989), Barbuy et al. (1991), and Milone & Barbuy (1994). The list of FeH lines is described in Schiavon et al. (1997). The line lists and corresponding molecular constants for the TiO  $\gamma'$ ,  $\delta$ ,  $\epsilon$  and  $\phi$  systems, adopted from Jorgensen (1994), are discussed in Section 4.

The photospheric models employed are from Kurucz (1992), Plez et al. (1992) and further unpublished models by Plez (1997), and Allard & Hauschildt (1995). The values of effective temperatures, surface gravities and metallicities adopted in the grid of models are reported in Table 4 (Sec. 5). Microturbulent velocities adopted were  $v_t = 1.0\text{km/s}$  and  $2.5\text{km/s}$  for  $\log g \geq 3.0$  and  $\log g \leq 2.5$  respectively. The Plez et al. (1992) grid, which was employed in the computation of spectra in the range  $2500 \leq T_{\text{eff}} \leq 3400$  K is only available for  $[\text{Fe}/\text{H}]=0.0$ , so that for  $[\text{Fe}/\text{H}] = -0.3$  and  $-0.6$  we have used the models for  $[\text{Fe}/\text{H}]=0.0$ , and the nonsolar metallicities were taken into account only in the input elemental abundances.

The calculations were carried out in steps of  $0.02\text{\AA}$  and the resulting spectra were rebinned to a step of  $1\text{\AA}$  and convolved with a gaussian function simulating an instrumental profile of  $\text{FWHM}=2\text{\AA}$ . We note that for the M giants studied here, it is important to take into account, in the calculation of continuum opacity, the  $\text{H}_2$  formation, which reduces the opacity due to HI and HII species.

The photospheric C and N values are modified in giants due to convective mixing so that we adopted  $[\text{C}/\text{Fe}] = -0.2$  and  $[\text{N}/\text{Fe}] = +0.4$  for giants of  $\log g \leq 2.0$ , and solar ratios for higher gravity stars. The change in C and N affects the TiO and CN bands: CN bands become stronger and, because of C deficiency, TiO bands also become stronger, since there is less CO association.

#### 4. TiO BANDS AND THE $T_{eff}$ SCALE OF M GIANTS

TiO bands are the main opacity source in the atmospheres of stars cooler than 4000K in the spectral region under study, and M giants are the dominant contributors to the integrated light of metal-rich and old composite systems such as bulge globular clusters and normal galaxies in the NIR.

In Figure 1 are shown the contributions of the most important electronic systems of TiO in the studied spectral region, for a star of  $T_{eff}=3200K$ ,  $\log g=0.0$  and  $[Fe/H]=-0.3$ . For  $\lambda \lesssim 8000 \text{ \AA}$ , the opacity is dominated by the  $\gamma$  and  $\gamma'$  systems, whereas for  $\lambda \gtrsim 8000 \text{ \AA}$ , the  $\delta$  and  $\epsilon$  systems are dominant, the opacity due to the  $\phi$  system being important only for  $\lambda \gtrsim 10000 \text{ \AA}$ .

The synthesis of the  $\gamma$  system was already presented in Milone & Barbuy (1994): the laboratory line list by J.G. Phillips (see Phillips 1973) is used, and Hönl-London and Franck-Condon factors were computed following the equations given by Kovacs (1979) and Bell et al. (1979) respectively; the electronic oscillator strength  $f_{el}$  adopted here is given in Table 3 and discussed in Sec. 4.2. We have chosen to use the laboratory line list because it reproduces better the shape of the (0,0)  $\gamma$  system bandhead (see discussion in Sec. 4.2.1).

The line lists used for the computation of the  $\gamma'$ ,  $\delta$ ,  $\epsilon$  and  $\phi$  systems, including the normalized product of the Franck-Condon and Hönl-London factors, were the ones computed by Jorgensen (1994), which were kindly made available to us by R. Bell. For these systems, while the Hönl-London and Franck-Condon factors were adopted directly from Jorgensen (1994), we derived electronic oscillator strengths  $f_{el}$  values by fitting the main vibrational bands in the spectra of M giants.

The fit to the intensity of TiO bandheads was applied to M stars of known stellar parameters ( $T_{eff}$ ,  $\log g$ ,  $[Fe/H]$ ,  $v_t$ ): two well-known field M giants and M giants along the

cool red giant branch of the metal-rich globular cluster NGC 6553. We searched for VO bands in our spectra by following identifications by Barnbaum et al. (1996), and found no evidence for the presence of these bands, even for the coolest stars of our sample. The determination of the oscillator strengths proceeded in two steps, described in detail in the subsections below: (a) fine-tuning of the effective temperature of cool giants of NGC 6553, based on their TiO  $\gamma$  system bandheads; (b) derivation of electronic oscillator strengths of the  $\gamma'$ ,  $\epsilon$ ,  $\delta$  and  $\phi$  systems, by fitting their main bandheads, adopting the temperatures established in (a).

#### 4.1. Stellar parameters for M giants of NGC 6553

In a detailed analysis of individual stars of NGC 6553, Barbuy et al. (1997) obtained a metallicity  $[\text{Fe}/\text{H}] = -0.35$  and a titanium-to-iron abundance ratio of  $[\text{Ti}/\text{Fe}] \approx +0.3$ . In a further analysis of these data, Barbuy et al. (1998) have confirmed that, in spite of a temperature uncertainty of 200 K,  $[\text{Ti}/\text{H}] \approx 0$  is found in all cases. As also discussed in Bruzual et al. (1997), a metallicity of  $[\text{Fe}/\text{H}] = -0.3$  to  $-0.4$  combined to enhanced  $[\alpha\text{-elements}/\text{Fe}] = +0.3$  to  $+0.4$  result in  $Z/Z_{\odot} \approx 1$  or  $[\text{M}/\text{H}] \approx 0$ . Furthermore, given that in our calculations the TiO bands are the dominant feature, and that  $[\text{Ti}/\text{H}] \approx 0$  is found for NGC 6553, it is clear that an overall metallicity  $[\text{M}/\text{H}] = 0.0$  is to be used. In conclusion, we adopt  $[\text{Fe}/\text{H}] = 0.0$  for NGC 6553, where by  $[\text{Fe}/\text{H}]$  we mean in fact  $[\text{M}/\text{H}]$ .

For our sample of M giants, temperatures are first derived from the (V–K) colours given in Guarnieri et al. (1998). In Table 2 are given the observed (V–K), for which reddening corrections were applied using  $E(\text{B–V}) = 0.7$  and  $E(\text{V–K})/E(\text{B–V}) = 2.744$  (Rieke & Lebofsky 1985), and temperatures derived through the calibration of Ridgway et al. (1980), LCB98 and BCP98.



The  $\gamma$  system bandheads were used to establish our  $T_{\text{eff}}$  scale for the cool stars, given that among the TiO systems considered in this work, it presents the best settled molecular constants available.

#### 4.1.1. Fits to reference stars

The fit to the field M giant HR 625, shown in Fig. 2, resulted in stellar parameters  $(T_{\text{eff}}, \log g, [\text{Fe}/\text{H}]) = (3600, 1.0, 0.0)$ . This  $T_{\text{eff}}$  is  $\sim 150\text{K}$  lower than the one estimated by Schiavon et al. (1997), on the basis of the spectral type M2 (Hoffleit & Warren, 1991) and the calibration by Fluks et al. (1994). In fact, the fit of the FeH bands in this star, adopting  $T_{\text{eff}} = 3750\text{ K}$  was not very satisfactory in Schiavon et al. (1997).

The fit to the vibrational sequence  $\Delta v = 0$  ( $v', v''$ ) = [(0,0), (1,1), (2,2), (3,3), etc.] ‘composite bandhead’ of the  $\gamma$  system at  $\lambda 7150\text{ \AA}$  to the spectra of stars in NGC 6553 (Table 2), was applied in a fine-tuning of their effective temperatures, which are given in the column 8 of Table 2. For each  $T_{\text{eff}}$  we adopted a surface gravity based on the  $T_{\text{eff}} \times \log g$  relation given by LCB98, which is based on the evolutionary tracks of Schaller et al. (1992) for  $1 M_{\odot}$  (column 9 of Table 2).

The  $T_{\text{eff}}$  estimations given in Table 2 indicate that (i) temperatures from the (V–K) empirical fits of BCP98 are lower than those derived from the theoretical values of their Table 5; (ii) our TiO-based effective temperature estimations show a good agreement with the resulting temperatures from (V–K) calibrations by Ridgway et al. (1980), LCB98 and BCP98 (empirical). The  $T(\text{TiO})$  values are adopted here. Taking into consideration the uncertainties in metallicity and  $\log g$ , we estimate an error of  $\Delta T_{\text{eff}} = 150\text{K}$  for the stars hotter than  $T_{\text{eff}} \sim 3200\text{K}$ , for which the gravity effect on band intensities is minimum (see discussion on Sect. 5). For cooler stars, gravity effects are more important, so that

uncertainties can reach  $\Delta T_{\text{eff}}=250\text{K}$ . Let us note that for  $T_{\text{eff}} \lesssim 3200\text{ K}$ , the TiO  $\gamma$   $\Delta v=0$  bandhead becomes saturated, so that for the star 291 (V12) the derived temperature is less precise - see also discussion on saturation of TiO bands in Sec. 5.

In Fig. 3 the fit of a synthetic spectrum of the  $\Delta v=0$  vibrational sequence of the  $\gamma$  system to the star 288 of NGC 6553 ( $T_{\text{eff}} = 3400\text{ K}$ ) is shown.

#### 4.2. Electronic oscillator strengths for the TiO $\gamma'$ , $\epsilon$ , $\delta$ and $\phi$ systems

The final  $f_{el}$  values obtained are given in Table 3, together with other determinations collected from the literature: the values by Davis et al. (1986) were obtained from correlations between equivalent widths of rotational lines and lifetime estimates for the  $\alpha$  and  $\beta$  systems; Brett (1990) obtained semi-empirical values through the fit of observed spectra of M giants; Jorgensen (1994) reports  $f_{el}$  values used in his calculations; Hedgecock et al. (1995) derived  $f_{el}$  from lifetime measurements; Langhoff (1997) ones were obtained from *ab initio* calculations; Alvarez & Plez (1998) present updated  $f_{el}$  values from recent laboratory measurements or calculations, which they also checked through comparisons between observed and calculated spectra of M giants.

The  $f_{el}$  values used in our calculations were derived in this work as follows:

(a) Adopting the  $T_{\text{eff}}$ s as described in Sec. 4.1, we derive  $f_{el}$  values for the  $\epsilon$  and  $\delta$  systems, by fitting the observed intensity of their  $\Delta v=0$  vibrational bands, as shown in Fig. 4. In the case of the  $\epsilon$  system, we had to shift the wavelengths of all lines by  $\Delta\lambda = +76.0\text{ \AA}$  in order to correctly reproduce the position of the (0,0) bandhead at  $\approx \lambda 8400\text{ \AA}$ . This  $\lambda_0$  shift is compatible with an uncertainty of the order of  $100\text{ cm}^{-1}$  in the electronic term  $T_e$  of the upper level ( $E^3\Pi$ ) of the transition (see Jorgensen 1994; Huber & Herzberg 1979; Simard & Hackett 1991). We find  $T_e = 11829.3$  for the  $E^3\Pi$  level, by shifting Jorgensen's

value. The value obtained for this system ( $f_{el} = 0.07$ ) is in disagreement with all values in the literature by a factor  $> 10$ . Recent laboratory determinations by Lundevall (1998) give a lifetime of  $4.0 \pm 0.2 \mu\text{s}$  for the  $E^3\Pi$  level, wherefrom a  $f_{el}$  even lower than Langhoff's would be derived. Therefore we preferred to omit our result for the  $\epsilon$  system in Table 3. For our purposes of computing a library of synthetic spectra, it is only important that the combination of line list, Franck-Condon factors, Hönl-London factors and  $f_{el}$  match the observed spectra. We suggest that the line list of Jorgensen (1994) for the  $\epsilon$  system is to be revised.

(b) The intensity of the vibrational sequences given by  $\Delta v = 0$  [( $v', v''$ )=(0,0), (1,1), (2,2), (3,3), etc.] and  $\Delta v = -1$  [( $v', v''$ )=(0,1), (1,2), (2,3), etc.] of the  $\gamma'$  system, at  $\approx 46200$  and  $46700 \text{ \AA}$  respectively, were used to obtain its electronic oscillator strength  $f_{el}$ , by fitting the spectrum of HR 625.

(c) The  $f_{el}$  of the  $\phi$  system was adopted from the ratio of the theoretical  $f_{el}$ s derived by Langhoff (1997) for the  $\delta$  and  $\phi$  systems, giving  $f_{el}^\phi / f_{el}^\delta \sim 0.2$ .

We adopted the procedure of fitting the bands from the different systems to the spectrum of the star NGC6553-288, for which the  $T_{\text{eff}}$  determined from the intensity of the bands from the  $\gamma$  system is in best agreement with the  $T_{\text{eff}}$ s derived from the various colours. The  $f_{el}$ s so derived for the other systems resulted in good fits to the spectra of all the remaining stars, of Table 2, adopting  $T(\text{TiO})$ .

The values derived in this work are in most cases similar to the average of the values estimated by other authors. The agreement between different authors is best for the  $\delta$  system. For the  $\gamma$  system, our adopted value of  $f_{el} = 0.12$  corresponds essentially to a mean of the laboratory values  $f_{el} = 0.165$  and  $0.092$  by Davis et al. (1986) and Langhoff (1997).

#### 4.2.1. Errors in the electronic oscillator strenghts

The main sources of uncertainty in the derivation of our astrophysical  $f_{el}$ s are the uncertainties in  $T_{\text{eff}}$ ,  $\log g$ , Ti and O abundances and the adopted microturbulent velocity ( $v_t$ ). Another potential source of uncertainties is a possible incompleteness in the laboratory line list adopted for the  $\gamma$  system. The latter is an important issue given that the  $f_{el}$ s of all the remaining systems are tied to the  $T_{\text{eff}}$ s derived from the intensities of the bands of the  $\gamma$  system.

We have adopted a fixed  $v_t = 2.5 \text{ km/s}$  for giants. For  $v_t = 1.5 \text{ km/s}$  there would occur an increase in the estimated  $f_{el}$  of 15%.

The uncertainty in the C and N abundances is estimated by computing the  $\gamma$  band with  $[\text{C}/\text{Fe}] = [\text{N}/\text{Fe}] = 0.0$ : the change relative to the adopted values of  $[\text{C}/\text{Fe}] = -0.2$  and  $[\text{N}/\text{Fe}] = 0.4$  is of the order of 2% in the estimated  $f_{el}$  value.

Adopting either a  $T_{\text{eff}}$  or a metallicity differing in 200K and 0.3dex respectively results in a shift of 20% in the resulting  $f_{el}$ s. As the  $\log g$  sensitivity of the TiO bands at  $T_{\text{eff}} \sim 3400\text{K}$  is very low (see Sec.5), the influence of this parameter upon the derived  $f_{el}$ s is very weak. An error of 0.5dex in  $\log g$  results in a difference of only 4% in the resulting  $f_{el}$ s. Taking into consideration all the above sources, the final uncertainty in our  $f_{el}$  values is around 30%.

We also computed synthetic spectra using the theoretical line list from Jorgensen (1994) for the  $\gamma$  system, in order to check for a possible incompleteness of the Phillips laboratory line list. As a result, the  $f_{el}$  that should be adopted with the Jorgensen line list is only marginally lower (8%) than the one that is compatible with the Phillips line list. Taking into consideration the other sources of uncertainty discussed above, we conclude that such an incompleteness in the Phillips line list has only a mild effect in our analysis.

Moreover, we chose to adopt the Phillips line list because it gives a better reproduction of the band shapes. The Jorgensen line list gives too high opacities at high  $J$  and too low opacities near the bandheads, so that it is very difficult to correctly reproduce the whole observed band shapes when employing this line list.

The use of the  $f_{el}$  value by Langhoff (1997) or Hedgecock et al. (1995), which are lower than ours by respectively 30% and 50%, would imply too low temperatures in comparison to those derived from the photometry (see below). We consider that these values are incompatible with our data.

## 5. A GRID OF SYNTHETIC SPECTRA: TiO vs. STELLAR PARAMETERS

We have computed a grid of synthetic spectra for the stellar parameters indicated in Table 4. A list of indices which measure TiO bands, as detailed in Table 5, was measured for the whole grid of spectra, in order to study their behavior as a function of stellar parameters.

In Fig. 5 are shown the plots of equivalent widths of TiO bands measured (cf. Table 5), for different  $\log g$  and for a fixed metallicity  $[\text{Fe}/\text{H}] = -0.3$ , as a function of  $T_{\text{eff}}$ . The bandheads at  $\lambda$  6000, 6600, 7150, 7600 and 8400 Å show similar behaviors, as expected. The dependence on gravity is also shown. In Fig. 6 the behavior of the indices, for a fixed  $\log g = 0.0$ , and different  $[\text{Fe}/\text{H}]$ , as a function of  $T_{\text{eff}}$ , shows the strong dependence on metallicity.

The  $\text{TiO}_2$  index as defined in Burstein et al. (1984) (Figs. 5b and 6b) is much less sensitive to surface gravity than  $\text{EW}_{6000}$ . In order to explain this, we plot in Fig. 7 the synthetic spectra for  $T_{\text{eff}} = 3400$  K,  $\log g = 0.5$  and  $[\text{Fe}/\text{H}] = 0.0$ , where the  $\text{TiO}_2$  index as

defined by Worthey et al. (1994) (the index is slightly modified relative to Burstein et al. 1984), as well as our  $EW_{6000}$  index are indicated (see also Table 5). It can be seen that the  $TiO_2$  index measures the bottom of the  $TiO \Delta v=0$  vibrational sequence of the  $\gamma'$  system, where line saturation is stronger. The index is clearly saturated for  $T_{\text{eff}} \lesssim 3500$  K (for  $[Fe/H] = 0.0$ ), so that its sensitivity to both  $T_{\text{eff}}$  and  $\log g$  is very small in this  $T_{\text{eff}}$  range – see Fig. 6b.

Figs. 5a-f and 6a-f show that the redder the  $TiO$  feature, two effects occur: the threshold of detection of the bands starts at progressively lower temperatures, and the bandheads saturate for cooler temperatures. For example,  $EW_{6000}$  and  $EW_{8400}$  rise in strength for  $T_{\text{eff}} \gtrsim 4000$  and  $3400$  K whereas saturation occurs at  $T_{\text{eff}} \lesssim 3000$  and  $\lesssim 2750$  K respectively. It has to be noted that in all plots of Figs. 5 and 6 the equivalent width corresponding to  $T_{\text{eff}}=2500$  K is underestimated, due to the use of  $\log g = -0.5$ , instead of  $\log g = -1.0$ , more appropriate for this temperature, since no models are available for  $\log g = -1.0$  in the Plez grid.

One conclusion that can be drawn from these plots is that for composite stellar populations of different mean temperatures, the use of different indices among those listed in Table 5 will be more appropriate in each case. For a very metal-rich and cooler stellar population of a massive elliptical galaxy,  $EW_{8400}$  would be more sensitive to changes in line strength, whereas for a metal-poor globular cluster the bluer indices are more suitable.

Fig. 8 shows the  $\Delta v=+1$  vibrational sequence of the  $\delta$  system, fitted to HR 3816. The features are clearly visible, although much weaker than the bluer ones, even for such a low temperature as  $T_{\text{eff}} = 2750$  K. The behavior of the corresponding index  $EW_{9800}$  vs.  $T_{\text{eff}}$  (Fig. 9) indicates that this band essentially does not saturate in the temperature range considered.

### 5.1. Integrated spectrum of NGC 6553

We concentrate our attention on the bulge cluster NGC 6553, for which we have a wealth of information: *i*) V and I photometry from the Hubble Space Telescope (Ortolani et al. 1995); *ii*) J and K photometry from the ESO 2.2m telescope (Guarnieri et al. 1998), resulting in reliable determinations of reddening and distance to the cluster; *iii*) detailed abundance analyses of stellar members (Barbuy et al. 1998), giving  $[\text{Fe}/\text{H}] \sim -0.4$  and  $[\alpha/\text{Fe}] \sim +0.4$ ; *iv*) medium-resolution spectra of stars from the tip of the red giant branch (Sec. 2) in the NIR, including several TiO bands, and *v*) the integrated cluster spectrum covering the spectral interval  $\lambda\lambda$  6000 – 9700 Å.

From the observed CMD, it is possible to compute the integrated synthetic spectrum of NGC 6553 in a straightforward manner. Such method was employed by de Souza et al. (1993), Barbuy (1994) and Milone et al. (1995) where synthetic spectra were used, and Santos et al. (1995) where the stellar library of Jacoby et al. (1984) was adopted. On the other hand, the integrated spectrum of NGC 6553 was reproduced in Bruzual et al. (1997), by using isochrones and several spectral libraries (synthetic and observed).

The CMD of NGC 6553 was transformed into a  $\log g \times T_{\text{eff}}$  diagram, using the  $T_{\text{eff}} \times \log g \times [\text{Fe}/\text{H}] \times (V-I)$  relations from BCP98 for all the stars, except the ones at the RGB tip. For the latter, we adopted the  $T_{\text{eff}}$  scale derived in Section 4. For the stars below the turn-off, we adopted a Salpeter IMF plus the M-dwarf theoretical main sequence from Baraffe et al. (1995). Each star in the  $\log g \times T_{\text{eff}}$  plane has its absolute I magnitude (computed from distance and reddening estimated by Guarnieri et al. 1998), and a corresponding synthetic spectrum, which is chosen to be the one with closest atmospheric parameters. The integrated synthetic spectrum is then obtained by summing up all the selected individual stellar spectra, weighted by  $M_I$ . In Fig. 10 the result is compared with the observed integrated spectrum of NGC 6553, adopting  $[\text{M}/\text{H}] = 0.0$ .

From the above calculations, we can estimate the contribution of stars from all evolutionary stages to the integrated light of the cluster. This is shown in Fig. 11, where it can be seen that the few stars in the RGB tip largely dominate the cluster light in the spectral region under consideration.

We note that the implementation of this grid of synthetic spectra to the code of evolutionary populations synthesis by Bruzual & Charlot (1998) is under way.

## 6. CONCLUSIONS

We present a new grid of synthetic spectra in the interval  $\lambda\lambda$  6000–10200Å. This grid is computed by employing state of the art model atmospheres and has a higher resolution than the ones currently in use in stellar population synthesis in the same spectral interval.

A fit to NIR spectra of stars from the RGB tip of NGC 6553 enabled us to derive a  $T_{\text{eff}}$  scale for the M giants, based on the TiO  $\gamma$  system band intensities, on the one hand, and also to determine a set of semi-empirical electronic oscillator strengths for the  $\gamma'$ ,  $\delta$ ,  $\epsilon$  and  $\phi$  systems of the TiO molecule.

The adequacy of our spectral library for stellar population synthesis purposes was tested for the case of NGC 6553, a well studied bulge globular cluster, for which detailed abundance analyses of individual stars and well-defined CMDs are available. In this framework, we obtained a good match to the ISED of this cluster. This result warrants the use of our spectral grid in stellar population synthesis studies in the NIR.

The authors are indebted to Robert Kurucz, France Allard and Bertrand Plez for providing their model atmospheres, Roger Bell for the theoretical TiO line list and for helpful comments, and to Michael Bessell for making available his results in advance of



publication. The anonymous referee is acknowledged for his helpful suggestions. All the computations were carried out in a DEC-Alpha 3000/700 workstation. RPS acknowledges the FAPESP PhD fellowship n<sup>o</sup> 93/2177-0.

## REFERENCES

- Allard, F., Hauschildt, P.H.: 1995, ApJ, 445, 433 (AH95)
- Alvarez, R. & Plez, B., 1998, A&A, 330, 1109.
- Baraffe, I., Chabrier, G., Allard, F. & Hauschildt, P.H., 1995, ApJ, 446, L35.
- Barbuy, B., 1982, PhD thesis, Université de Paris VII.
- Barbuy, B. 1985, A&A, 151, 189
- Barbuy, B. 1994, ApJ, 430, 218
- Barbuy, B., Spite, M., Spite, F., Milone, A.: 1991, A&A, 247, 15
- Barbuy, B., Castro, S., Ortolani, S. & Bica, E., 1992, A&A, 259, 607.
- Barbuy, B., Ortolani, S., Bica, E., Renzini, A., Guarnieri, M.D.: 1997, in IAU Symp. 189, *Fundamental stellar parameters: confrontation between observation and theory*, eds. T. Bedding, A. Booth & J. Davis, Kluwer Acad. Pub., p. 203
- Barbuy, B., Renzini, A., Ortolani, S., Bica, E., Guarnieri, M.D. 1998, in preparation
- Barnbaum, C., Omont, A., Morris, M. 1996, A&A, 310, 259
- Bell, R.A., Dwivedi, P.H., Branch, D. & Huffaker, J.N., 1979, ApJS, 41, 593
- Bessell, M.S., Castelli, F., Plez, B. 1998, A&A, 333, 231 (BCP98)
- Bica, E., Alloin, D. 1986, A&A, 162, 21
- Brett, J.M. 1990, A&A, 231, 440
- Bruzual, G., Charlot, S.: 1998, in preparation
- Bruzual, G., Barbuy, B., Ortolani, S., Bica, E., Cuisinier, F., Lejeune, T., Schiavon, R. 1997, AJ, 114, 1531
- Burstein, D., Faber, S.M., Gaskell, C.M., Krumm, N. 1984, ApJ, 287, 586

- Davis, S.P., Littleton, J.E. & Phillips, J.G., 1986, *ApJ*, 309, 449.
- Delbouille, L., Roland, G., Neven, L. 1973, *Photometric Atlas of the Solar Spectrum from 3000 to 10000 Å*, Liège: Institut d'Astrophysique
- de Souza, R.E., Barbuy, B., dos Anjos, S. 1993, *AJ*, 105, 1737
- Erdelyi-Mendes, M., Barbuy, B. 1989, *A&AS*, 80, 229
- Fluks, M.A., Plez, B., Thé, P.S., de Winter, D., Westerlund, B.E., Steenman, H.C., 1994, *A&AS*, 105, 311.
- Grevesse, N., Noels, A., Sauval, J.: 1996, in *ASP Conf. Ser. 99*, eds. S.S. Holt, G. Sonneborn, p. 117
- Guarnieri, M.D., Ortolani, S., Montegriffo, P., Renzini, A., Barbuy, B., Bica, E., Moneti, A.: 1998, *A&A*, 331, 70
- Hamuy, M., Suntzeff, N.B., Heathcote, S.R., Walker, A.R., Gigoux, P. & Phillips, M.M., 1994, *PASP*, 106, 566.
- Hedgecock, L.M., Naulin, C., Costes, M., 1995, *A&A*, 304, 667.
- Hoffleit, D. & Warren Jr., W.H., 1991, *Preliminary Version of the Bright Star Catalogue*, 5th Revised Edition.
- Huber, K.P., Herzberg, G. 1979, *Constants of Diatomic Molecules*, van Nostrand, Toronto
- Jacoby, G.H., Hunter, D.A., Christian, C.A. 1984, *ApJS*, 56, 257
- Jorgensen, U.G.: 1994, *A&A*, 284, 179
- Kovacs, I. 1969, *Rotational Structure in the Spectra of Diatomic Molecules*, N. York, American Elsevier
- Kurucz, R. 1992, in *IAU Symp. 149, The Stellar Populations of Galaxies*, eds. B. Barbuy & A. Renzini, Kluwer Acad. Pub., p. 225 (K92)

- Langhoff, S. 1997, *ApJ*, 481, 1007
- Lejeune, T., Cuisinier, F., Buser, R. 1998, *A&AS*, 130, 65 (LCB98)
- Lundevall, C., 1998, *J.Mol.Spec.*, in press.
- Milone, A., Barbuy, B.: 1994, *A&AS*, 108, 449
- Milone, A., Barbuy, B., Bica, E. 1995, *A&AS*, 113, 547
- Ortolani, S., Barbuy, B., Bica, E. 1990, *A&A*, 236, 362
- Ortolani, S., Renzini, A., Gilmozzi, R., Marconi, G., Barbuy, B., Bica, E. & Rich, R.M. 1995, *Nature*, 377, 701.
- Phillips, J.G. 1973, *ApJS*, 26, 313
- Plez, B. 1997, private communication (P97)
- Plez, B., Brett, J.M., Nordlund, A. 1992, *A&A*, 256, 551 (PBN92)
- Ridgway, S.T., Joyce, R.R., White, N.M., Wing, R.F. 1980, *ApJ*, 235, 126.
- Rieke, G.H., Lebofsky, M.J. 1985, *ApJ*, 288, 618.
- Schiavon, R.P., Barbuy, B., Singh, P.D.: 1997, *ApJ*, 484, 499.
- Simard, B., Hackett, P.A. 1991, *J. Mol. Spec.* 148, 128.
- Santos Jr., J.F.C., Bica, E., Dottori, H., Ortolani, S., Barbuy, B. 1995, *A&A*, 303, 753.
- Spite, M. 1967, *Ann. Ap.* 30, 211
- Worthey, G., Faber, S.M., González, J.J., Burstein, D. 1994, *ApJS*, 94, 687.

Table 1. Log of the observations of field and cluster M giants.

star	V	$\alpha_{1950}$	$\delta_{1950}$	date	exp.(m)	$\lambda\lambda$ ( $\text{\AA}$ )
HR 625	6.10	02 <sup>h</sup> 06 <sup>m</sup> 23.4 <sup>s</sup>	-18°00'55.5"	05.08.96	2	5900-9200
HR 3816	6.10	09 30 59.2	-62 34 01	01.02.96	0.5	8090-10040
NGC 6553-int.	–	18 05 11	-25 55 06	19.07.96	30	5900-9200
NGC 6553-291	16.92	”	”	10.06.97	30	6865-8251
NGC 6553-125	15.89	”	”	”	”	6865-8905
NGC 6553-288	15.91	”	”	”	”	”
NGC 6553-47	15.35	”	”	”	”	”
NGC 6553-118	15.70	”	”	”	”	”
NGC 6553-211	15.61	”	”	”	”	”

Table 2. Frame coordinates, observed (V-K) colours and temperatures of 6 cool giants of NGC 6553. Coordinates correspond to the frame in K band shown in Fig. 1 by Guarnieri et al. (1998); star numbers and colours are also from Guarnieri et al. The field stars HR 625 and HR 3816 are also included in the Table. Relations colour-temperature by Bessell et al. (1998) - BCP (theoretical/empirical), Lejeune et al. (1998) - LCB98, and Ridgway et al. (1980) are used. Gravities adopted are given in the last column.

star	X	Y	(V-K)	$T_{BCP}$	$T_{LCB}$	$T_{Ridgway}$	$T_{TiO}$	log g
291/V12	-4.7	324.0	9.75	3250/3075	3100	3060	3200	0.0
125	30.1	276.5	7.21	3520/3476	3550	3530	3500	0.7
288	10.8	334.0	7.93	3420/3367	3400	3410	3400	0.5
47	63.7	286.2	6.96	3550/3518	3590	3570	3400	0.5
118	30.0	281.0	7.15	3530/3476	3550	3540	3500	0.7
211	14.1	224.9	3.89*	–	–	–	3500	0.7
HR 625	–	–	4.48	3660/3670	3700	3680	3600	1.0
HR 3816	–	–	–	–	–	–	2750	-0.5

Note. — \* For the star 211 the (V-K) colour appears to be in error, since the spectrum is incompatible with a high temperature

Table 3. Electronic oscillator strengths from the literature (Davis, Littleton & Phillips 1986 - DLP86; Brett 1990 - B90; Jorgensen 1994 - J94; Hedgecock, Naulin & Costes 1995 - HNC95; Langhoff 1997 - L97; Alvarez & Plez 1998 - AP98) compared to the value found in the present work

system	DLP86	B90	J94	HNC95	L97	AP98	This Work
$\gamma'$	0.138	—	0.14	0.093	0.108	0.0935	0.06
$\gamma$	0.165	0.22	0.15	0.079	0.092	0.0786	0.12
$\delta$	0.05	0.05	0.048	—	0.096	0.048	0.05
$\epsilon$	—	0.006	0.014	<0.0056	0.002	0.0023	—
$\phi$	0.05	0.05	0.052	—	0.018	0.0178	0.01

Table 4. Stellar parameters and corresponding photospheric models used to build the grid of synthetic spectra; models are from Kurucz (1992) - K92, Plez (1997) - P97, Plez et al. (1992) - PBN92 and Allard & Hauschildt (1995) - AH95

$T_{\text{eff}}/\text{step}$	$\log g/\text{step}$	[Fe/H]	models
4500-6000/250	0.0-5.0/0.5	-0.3,0.0	K92
4000-4500/250	2.0-5.0/0.5	-0.3,0.0	K92
4000-4500/250	0.0-1.5/0.5	-0.6,-0.3,0.0	P97
3600-4000/200	-0.5-1.0/0.5	-0.6,-0.3,0.0	P97
3000-3400/200	-0.5-1.5/0.5	-0.6,-0.3,0.0	PBN92
2750-3000/250	-0.5-1.5/0.5	-0.6,-0.3,0.0	”
2500	-0.5	-0.6,-0.3,0.0	”
2800-3200/200	3.5-5.0/0.5	-0.5,0.0	AH95
3300-3700/200	3.5-5.0/0.5	-0.5,0.0	”
2500	5.5	-0.5,0.0	”



Table 5. Definition of spectral indices measured

Index	$T_{eff}$ range	Blue continuum	Bandpass	Red continuum
$EW_{6000}$	$\leq 3600$	6143.95-6146.41	6145.18-6540.93	6539.58-6542.27
$EW_{6000}$	$\geq 3600$	6067.47-6074.81	idem	idem
$EW_{6600}$	$\leq 3600$	6539.58-6542.27	6540.93-7048.22	7548.70-7553.14
$EW_{6600}$	$\geq 3600$	idem	idem	7594.40-7598.00
$EW_{7100}$	$\leq 3600$	7046.36-7050.08	7048.22-7550.92	7548.70-7553.14
$EW_{7100}$	$\geq 3600$	6539.58-6542.27	idem	7594.40-7598.00
$EW_{7600}$	$\leq 3600$	7548.70-7553.14	7550.92-8190.40	8188.86-8191.93
$EW_{7600}$	$\geq 3600$	7593.64-7598.33	idem	8259.46-8261.50
$EW_{8400}$	$\leq 3600$	8188.86-8191.93	8190.40-8853.40	8850.67-8856.13
$EW_{8400}$	$\geq 3600$	8259.46-8261.50	idem	idem
$EW_{9800}$	—	9721.67-9725.00	9726.00-9972.00	9975.23-9981.52
$TiO_2$ (Burstein)	—	6069.00-6142.75	6192.00-6273.25	6375.00-6416.25
$TiO_2$ (Worthey)	—	6068.375-6143.375	6191.375-6273.375	6374.375-6416.875

### FIGURE CAPTIONS

Fig. 1.— Strongest TiO bands in the near infrared, corresponding to the  $\gamma$ ,  $\gamma'$ ,  $\epsilon$  and  $\delta$  electronic systems.

Fig. 2.—  $\gamma$  and  $\gamma'$  bandheads for HR 625. Solid lines: synthetic spectrum computed for  $T_{\text{eff}}=3600$  K,  $\log g = 1.0$ ,  $[\text{Fe}/\text{H}] = 0.0$ ; dashed line: observed spectrum

Fig. 3.—  $\Delta v=0$  and  $\Delta v=-1$  vibrational sequences of the  $\gamma$  system for the star NGC 6553:288. Solid line: synthetic spectrum computed with  $T_{\text{eff}}=3400$  K,  $\log g = 0.5$ ,  $[\text{Fe}/\text{H}] = 0.0$ ; dashed line: observed spectrum.

Fig. 4.—  $\Delta v=2$  vibrational sequence of the  $\gamma$  system,  $\Delta v=0$  of the  $\epsilon$  system and  $\Delta v=0$  of the  $\delta$  system for NGC 6553:288. Solid line: synthetic spectrum computed with  $T_{\text{eff}}=3400$  K,  $\log g = 0.5$ ,  $[\text{Fe}/\text{H}] = 0.0$ ; dashed line: observed spectrum.

Fig. 5.— TiO features vs.  $T_{\text{eff}}$  for  $[\text{Fe}/\text{H}] = -0.3$  and  $\log g = -0.5, 0.0, 0.5, 1.0$  and  $1.5$ .

Fig. 6.— TiO features vs.  $T_{\text{eff}}$  for  $\log g = 1.5$  and  $[\text{Fe}/\text{H}] = -0.6, -0.3$  and  $0.0$ .

Fig. 7.— Synthetic spectra for  $T_{\text{eff}} = 3400$  K,  $\log g = 0.5$  and  $[\text{Fe}/\text{H}] = 0.0$ , where the  $\text{TiO}_2$  index as defined according to Worthey et al. (1994), and our  $\text{EW}_{6000}$  index are indicated.

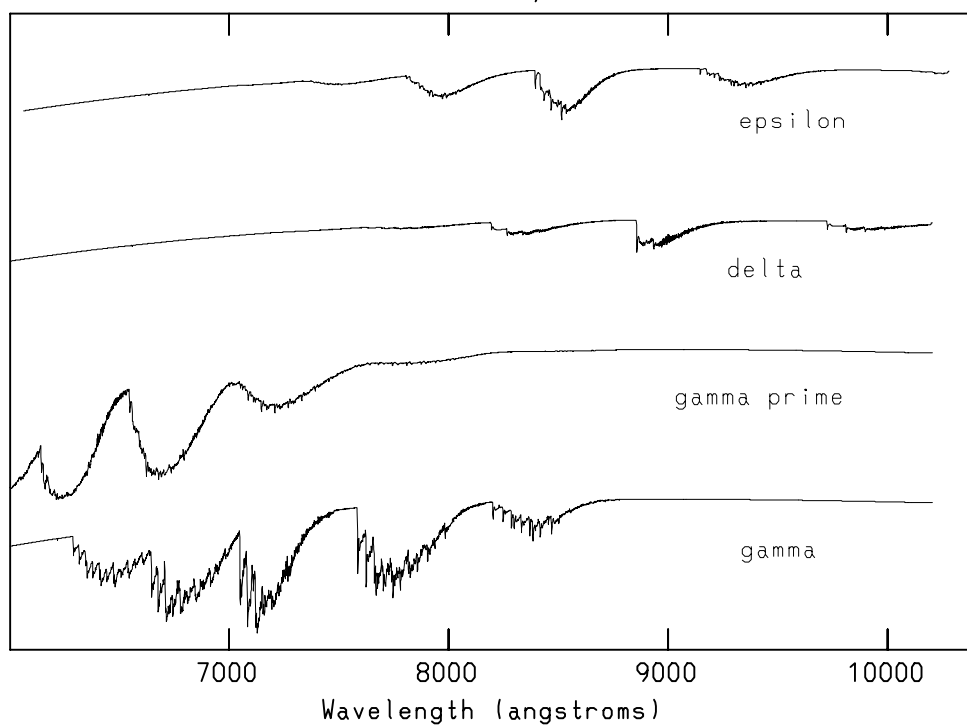
Fig. 8.—  $\Delta v = +1$  vibrational sequence of the  $\delta$  system in HR 3816. Solid line: synthetic spectrum computed for  $T_{\text{eff}}=2750$  K,  $\log g = -0.5$ ,  $[\text{Fe}/\text{H}] = 0.0$ ; dashed line: observed spectrum.

Fig. 9.— TiO feature  $\text{EW}_{9800}$  vs.  $T_{\text{eff}}$ . Symbols are as in Fig. 5 and open stars correspond to dwarfs.

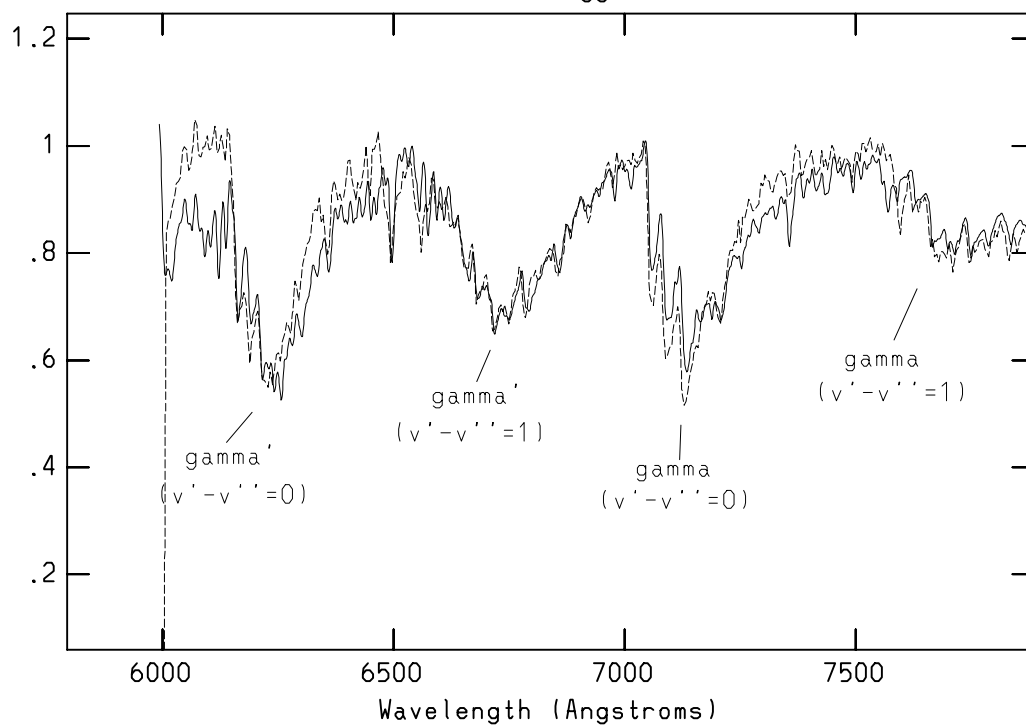
Fig. 10.— Integrated spectrum of NGC 6553. Dashed line: observed spectrum; solid line: synthetic spectrum computed as described in Sec. 5.1.

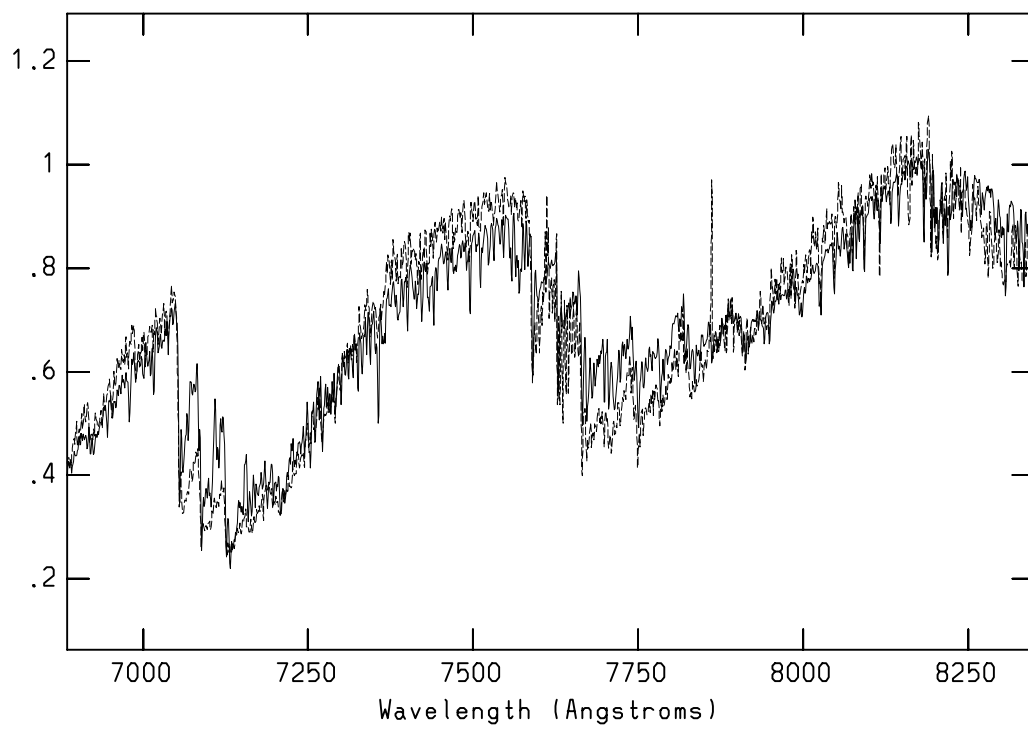
Fig. 11.— Contribution of stars in different evolutionary stages to the integrated light of NGC 6553.

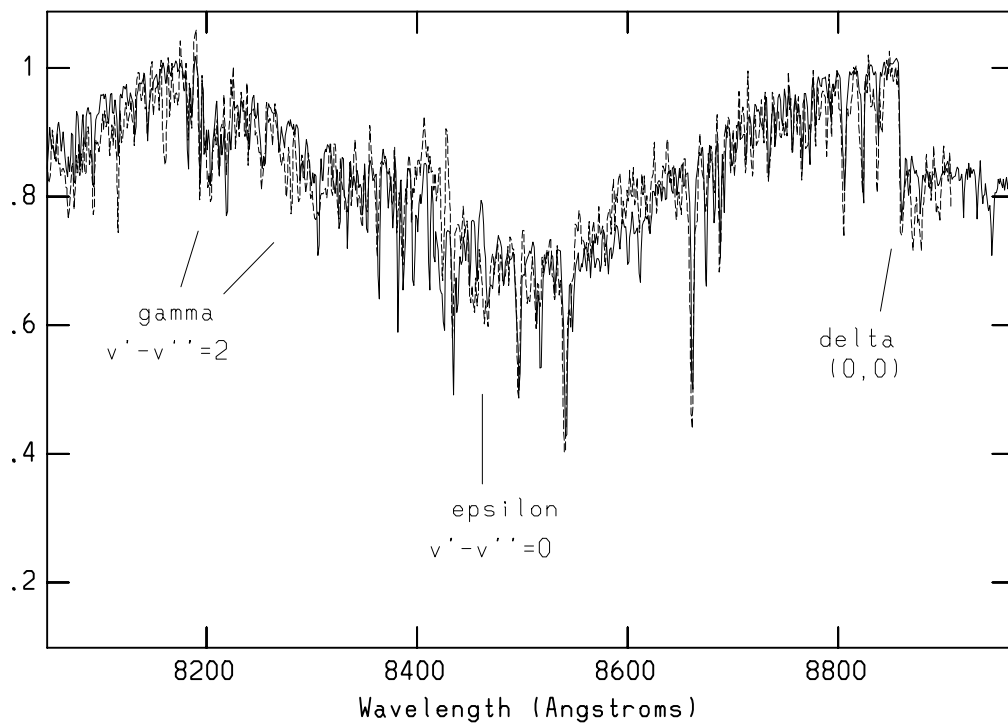
TiO relevant electronic systems for  $T_{\text{eff}}=3200\text{K}$



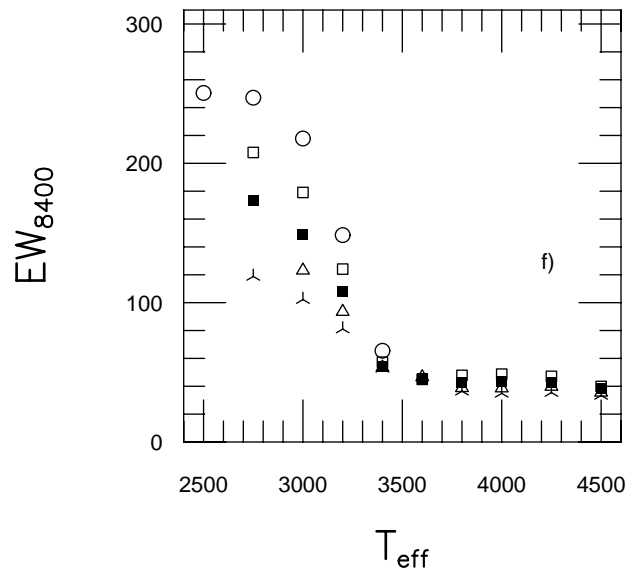
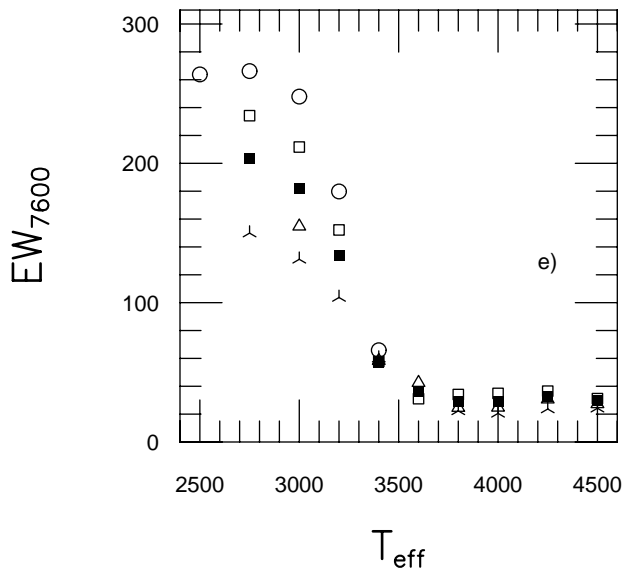
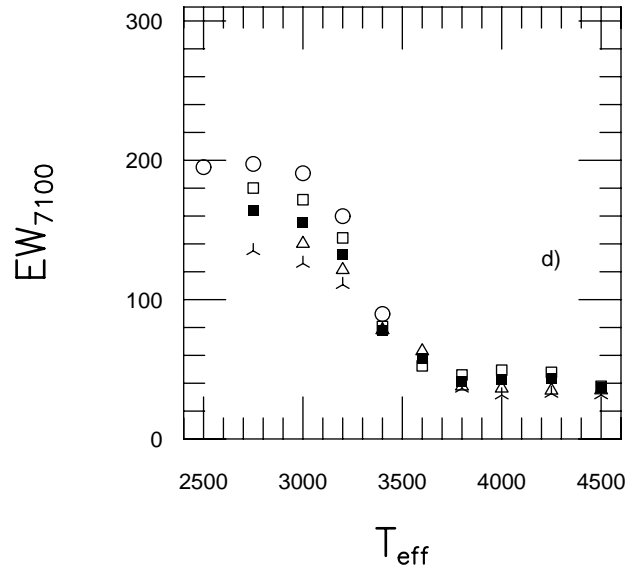
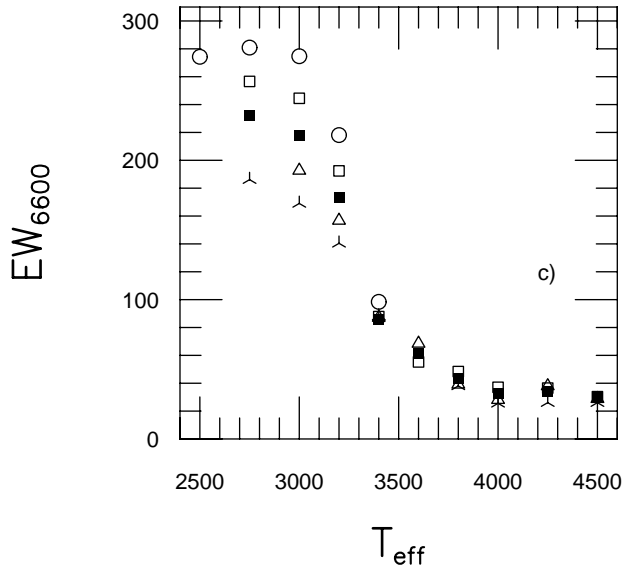
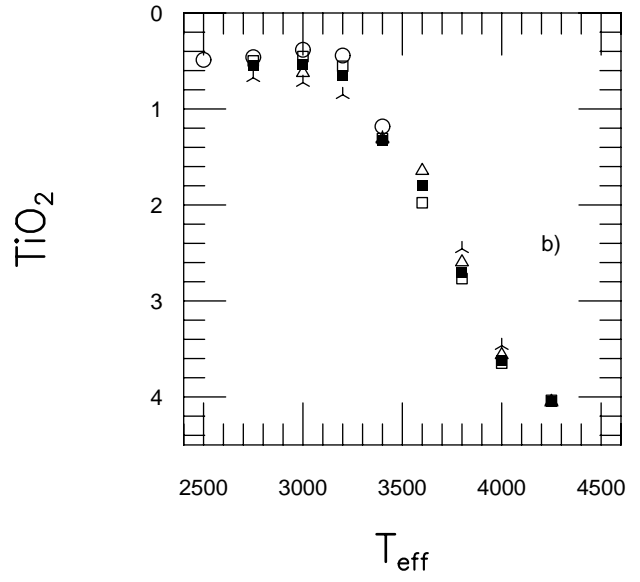
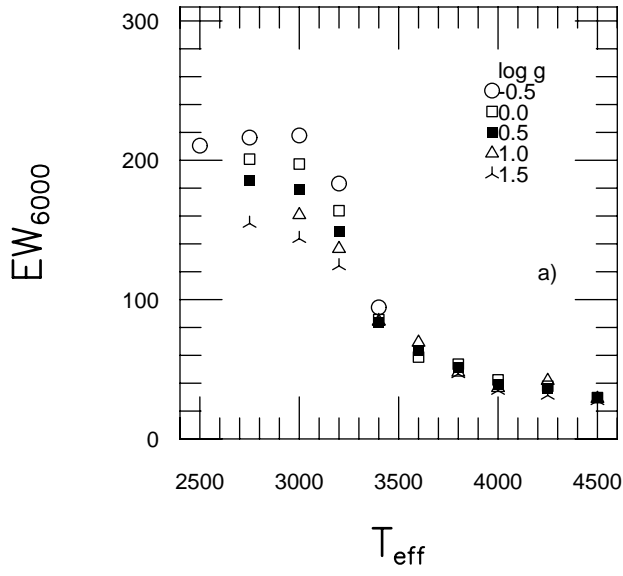
HR 625  $T_{\text{eff}}=3600\text{K}$   $\log g=1.0$   $[\text{Fe}/\text{H}]=0.0$







[Fe/H] = -0.3





$\log g = 0.0$

